FATIGUE CRACK PROPAGATION THROUGH AUSTEMPERED DUCTILE IRON MICROSTRUCTURE

Lukáš Bubenko[1], Radomila Konečná[1], Gianni Nicoletto[2]

Received 24th September 2010; accepted in revised form 18th October 2010

Abstract

Austempered ductile iron (ADI) has a wide range of application, particularly for castings used in automotive and earth moving machinery industries. These components are usually subjected to variable dynamic loading that may promote initiation and propagation of fatigue cracks up to final fracture. Thus, it is important to determine the fatigue crack propagation behavior of ADI. Since fatigue crack growth rate (da/dN) vs. stress intensity factor K data describe fatigue crack propagation resistance and fatigue durability of structural materials, da/dN vs. K_a curves of ADI 1050 are reported here. The threshold amplitude of stress intensity factor K_{ath} is also determined. Finally, the influence of stress intensity factor amplitude to the character of fatigue crack propagation through the ADI microstructure is described.

Keywords: *Austempered ductile iron; Fatigue; Stress intensity factor; Crack; Microstructure.*

1. Introduction

Even nowadays, in era of light alloys and composites, ductile iron (DI) still represents a structural material of choice for a wide range of demanding technical applications. Furthermore, the mechanical properties of DI can be significantly improved by a special heat treatment known as austempering that was first commercially applied to DI in 1970's [1, 2]. The conventional process consists of full austenization of the casting in the temperature range of 871 - 982 °C followed by quenching to an intermediate temperature (austempering temperature) range of 240 - 400 °C to avoid formation of pearlite. The casting is maintained at the austempering temperature for 2 - 4 h, depending on the section size, and finally cooled in air to room temperature [1-4].

The mechanical properties of austempered ductile iron (ADI) are closely related to the type of microstructure, which depends on a number of factors, the most important being the austempering temperature. High austempering temperatures result in improved ductility, fatigue and impact strengths and relatively low yield and tensile strengths. At low austempering temperatures, ADI displays high yield and tensile strengths, high wear resistance, but reduced ductility and impact strength [1, 5, 6].

Alloying elements in ADI are normally required for hardenability purposes or the austemperability of DI when section sizes are greater than 19 mm. The alloying elements that are typically added for hardenability purposes are Cu, Ni and Mo [2, 5].

The microstructure of ADI consists of acicular ferrite, that can be fine (characteristic for lower bainite produced at lower temperatures) or coarse (characteristic for upper bainite produced at higher temperatures), high carbon austenite and nodules of graphite particles [2, 4]. European

[1] L. Bubenko, Ing., R. Konečná, prof. Ing. PhD. - Department of Materials Engineering, Faculty of Mechanical Engineering, University of Žilina, Univerzitná 1, 010 26 Žilina, Slovak Republic.

[2] G. Nicoletto, prof. – Department of Industrial Enginnering, Università degli Studi di Parma, Viale G.P. Usberti, 181/A, 431 00 Parma, Italy.

[*]Corresponding author, e-mail address: lukas.bubenko@fstroj.uniza.sk

norm (EN) specifies four grades of ADI in dependence of the ultimate tensile strength (R_m), while American standard (ASTM) specifies five grades [1, 2].

Combination of properties, such as strength, ductility, fatigue resistance and wear resistance, makes ADI not only an engineering material that may substitute cast, forged and/or heat treated steels, but even aluminum in applications, where high strength/weight ratio is important. The major applications of ADI include gears, crankshafts, connecting rods, camshafts, engine mounts, transmissions, suspension components, sprockets, and many other parts used in automotive, railway, earth moving, excavating and agricultural equipment [1, 4, 6 - 9].

All of these mechanical components are generally subjected to the dynamic variable loading in service. To avoid unexpected failures, it is important to know the fatigue properties of the material and to be able to predict the fatigue life of the structural part. Linear elastic fracture mechanics presents one of the approaches to determine fatigue life of mechanical parts. In this approach, the crack propagation rate of long fatigue cracks can be expressed as a function of the stress intensity factor amplitude K_a. Therefore, experimental da/dN vs. K_a data are plotted in a bilogarithmic diagram and a fatigue crack propagation curve determined by data fitting.

The stress intensity factor amplitude is generally given by:

$$K_a = \sigma_a (\pi a)^{1/2} f\left(\frac{a}{W}\right), \quad [MPa.m^{1/2}] \tag{1}$$

where

σ_a [MPa] - the stress amplitude;

W [mm] - the specimen width;

a [mm] - the crack length.

At low values of K_a the fatigue crack propagation reaches rates of order of 10^{-10} m/cycle, i.e. the fatigue crack tends to arrest. This value of K_a is known as the threshold amplitude of stress intensity factor K_{ath}.

The objective of this investigation was thus to determine near-threshold fatigue crack growth behavior of an ADI material, observe fracture surface and fracture profile, and to describe the influence of K_a on the character of fatigue crack propagation.

2. Material and experimental procedure

The investigated material was ADI 1050 (EN-GJS-1000-5), an austempered ductile iron intended for production of cast components with high fatigue resistance. Basic mechanical properties are given in Table 1. Experimental material was delivered in the form of cast blocks by Zanardi Fonderie S.p.A., an Italian company specialized in the production of conventional DI and of ADI components. The main applications of tested ADI 1050 are earth movement undercarriage components, passenger vehicles suspension parts and crankshafts [10].

Tab. 1

Mechanical properties of ADI 1050 [10]

Material	HBW	R_m [MPa]	$R_{p0.2}$ [MPa]
ADI 1050	332	1090	770

The typical microstructure of ADI 1050 is shown in Fig. 1.

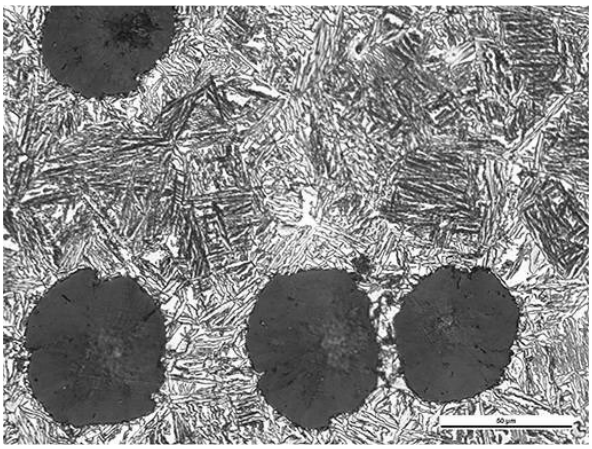

Fig. 1. The microstructure of ADI 1050, etched with 3 % Nital

Microstructure was formed by spheroidal graphite particles uniformly distributed in a matrix that consisted of thick acicular ferrite laths and retained high carbon austenite. This structure is characteristic for upper bainite. The determined results of nodule characterization are shown in Table 2.

Tab. 2

Nodule characteristics of ADI 1050

Material	Nodule count (mm^{-2})	Area fraction of nodule (%)	Nodularity (%)
ADI 1050	54	10.1	57.3

To determine the fatigue crack propagation behavior, compact tension (CT) specimens (Fig. 2) were prepared from supplied cast blocks as per ASTM standard [11]. The Chevron notched specimens were prepared with a thickness B = 10 mm and width of W = 50 mm. To achieve sufficient visibility of fatigue cracks using CCD cameras, both observed surfaces were polished by 1 micron grain size diamond paste.

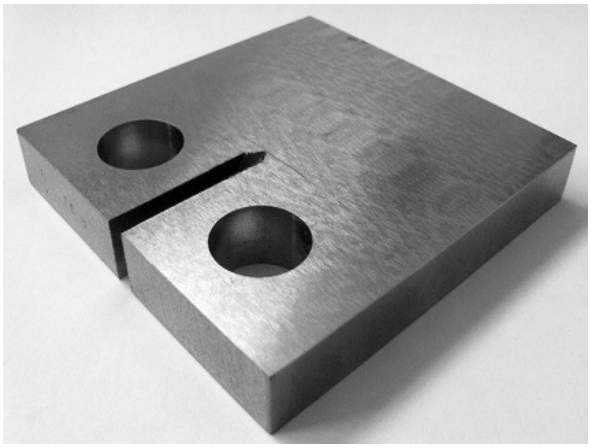

Fig. 2. Compact tension specimen

Fatigue crack growth rate tests were performed at IPM AS CR in Brno in accordance with ASTM standard [11]. Both the precracking and crack growth tests were conducted in an electromagnetic resonant test machine (Roell Amsler HFP 5100).

A sinusoidal waveform was applied and the load ratio was kept constant at R = 0.1. The crack lengths were monitored by using CCD cameras and measured by digital micrometers. Crack lengths on both sides of specimens, together with the number of cycles for crack propagation, were continuously recorded. All tests were performed at room temperature in ambient air conditions.

Three identical CT specimens were tested and the fatigue crack propagation curves da/dN vs. K_a were determined according to the ASTM standard [11]. The stress intensity factor amplitude K_a for CT specimens is given by equation:

$$K_a = \frac{P_a}{B\sqrt{W}} \frac{(2+\alpha)}{(1-\alpha)^{3/2}} \left(0.886+4.64\alpha-13.32\alpha^2+14.72\alpha^3-5.6\alpha^4\right), \quad \alpha = \frac{a}{W} \tag{2}$$

where B is the specimen thickness.

The threshold amplitude of stress intensity factor K_{ath} for fatigue crack propagation was determined using the load shedding technique [11]. This procedure involves slowly reducing the load values and recording the crack growth rate. Load shedding was done by reducing the stress intensity range stepwise after the crack had grown by at least 1 mm in length at the previous K_a level. The threshold was identified as the value of K_a at which the crack growth rate was of the order of 10^{-10}mm/cycle. The value of K_{ath} was then determined as the average value from measured data of two specimens.

After fatigue crack growth testing, the CT specimens were broken under tensile load. The structural analysis was carried out on polished sections, etched by 3 % Nital. Metallographic techniques and digital image analysis were applied in the NEOPHOT 32 optical microscope. Fractographic analysis of fatigue crack propagation mode within ADI 1050 microstructure was performed on scanning electron microscope TESCAN VEGA 3 SB.

3. Results and discussion

The fatigue crack propagation curves determined with three identical CT specimens of ADI 1050 are shown in Fig. 3, where the y axis is the logarithmic value of fatigue crack growth rate da/dN and the abscissa presents the logarithmic value of stress intensity factor amplitude K_a.

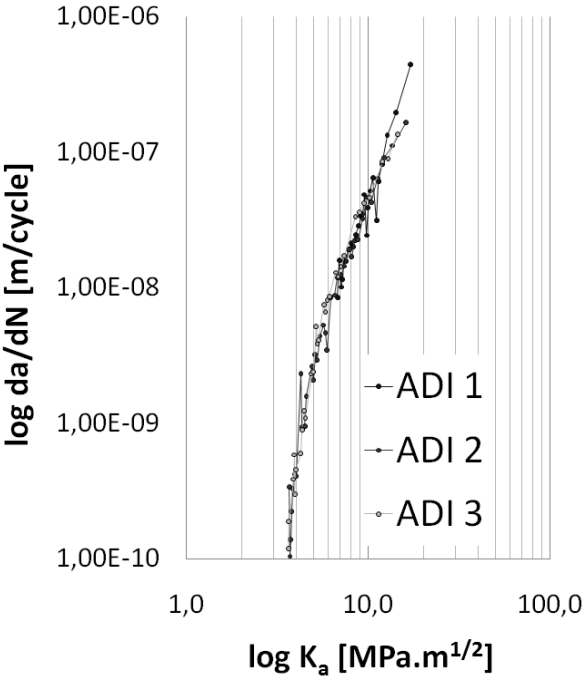

Fig. 3. Fatigue crack growth rate data of ADI 1050

Based on crack propagation curves, denominated as ADI 2 and ADI 3, the threshold value of stress intensity factor amplitude was determined as $K_{ath} = 3.8$ MPa.m$^{1/2}$. This value refers to crack propagation rate da/dN within 10^{-10} to 10^{-9}m/cycle, which practically represents the no-growth (or crack arrest) condition for a crack present in a mechanical component. This value is in good agreement with work of Yang and Putatunda [3], who achieved comparable results when investigated ADI with similar mechanical properties.

The influence of stress intensity factor amplitude K_a on the long fatigue crack propagation mode within the ADI 1050 specimens is visible in Fig. 4 and Fig. 5.

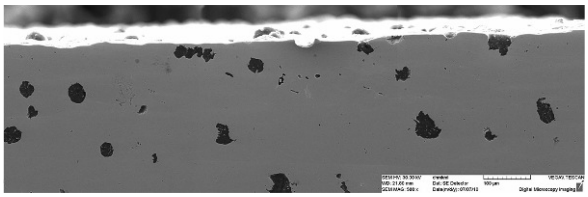

Fig. 4. Detail of fracture profile at $K_a = 4$ MPa.m$^{1/2}$

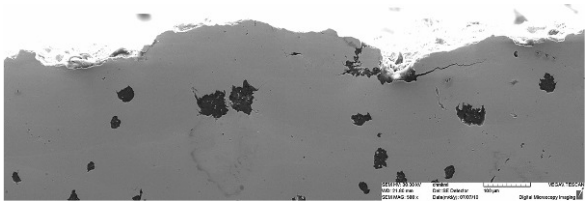

Fig. 5. Detail of fracture profile at $K_a = 14$ MPa.m$^{1/2}$

In the near threshold region where the stress intensity factor amplitude is of $K_a = 4$ MPa.m$^{1/2}$, i.e. at low crack propagation rates da/dN = 1.10^{-9}m/cycle, the crack has a linear straight character (Fig. 4) and grows approximately perpendicularly to the direction of the applied principal stress. However, at higher values of $K_a = 14$ MPa.m$^{1/2}$, i.e. at crack propagation rates of orders of 10^{-6}mm/cycle, the propagation mode tends to become more rugged and irregular (Fig. 5). Stokes et al. in their research have suggested the same influence of the stress intensity factor K on long crack propagation mode [12].

The fatigue fracture surface shows that the dominant mechanism for fatigue crack growth of ADI is quasi-cleavage. In general, the character of fractures is similar (Fig. 6 and Fig. 7).

Fig. 6 shows near threshold fatigue crack growth area ($K_a = 4$ MPa.m$^{1/2}$) with detail of a casting defect. As with Fig. 7, ductile striated crack growth along with isolated facets of cleavage mostly occurring in the vicinity of graphite nodules is observed. This combination of ductile striation and cleavage planes, whose river patterns go into tear rivers, is named quasi-cleavage [13]. This mechanism consists of the initiation of small cracks ahead of the main crack front, in a preferentially oriented plane that cleaves. These small cracks propagate radially,

first in the brittle manner that later becomes ductile striation, to finally join the main crack front [13].

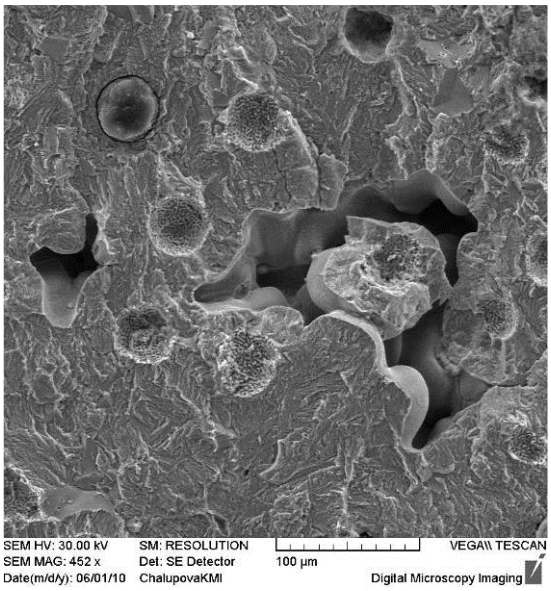

Fig. 6. Detail of fracture at K_a = 4 MPa.m$^{1/2}$

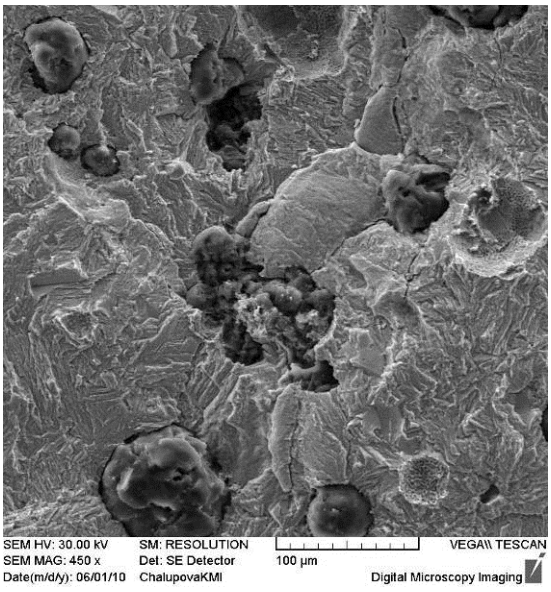

Fig. 7. Detail of fracture at K_a = 14 MPa.m$^{1/2}$

4. Conclusions

The aim of this investigation was to determine near threshold fatigue crack behavior of ADI 1050 and to study the mode of long fatigue crack propagation in dependence of stress intensity factor amplitude K_a. The following conclusions were reached:

- threshold stress intensity factor amplitude K_{ath} of material ADI 1050 is 3.8 MPa.m$^{1/2}$;
- the roughness of fracture profile increases with the stress intensity factor amplitude K_a as follows:
  - at near threshold when K_a = 4 MPa.m$^{1/2}$ (i.e. at low crack propagation rates da/dN = 1.10^{-9} m/cycle), the crack has a linear straight character and grows approximately perpendicularly to the direction of the applied principal stress;
  - at a high value of K_a = 14 MPa.m$^{1/2}$, (i.e. crack growth rates of about 10^{-6}mm/cycle), the propagation mode has a tendency to become more rugged and irregular;
- fatigue fracture mechanism is characterized by quasi-cleavage;
- decohesion of graphite particles from matrix often occurs.

Acknowledgements

This investigation was made with support of national project KEGA 3/6110/08 and VEGA 1/0242/10.

References

[1] R. A. Harding: Kovove Materialy, Vol. 45, 2007, No. 1, p. 1-16.

[2] K. L. Hayrynen: The production of Austempered Ductile Iron (ADI), World Conference on ADI, Louisville, Kentucky, cosponsored by Ductile Iron Society and the American Foundry Society, 2002.

[3] J. Yang, S. K. Putatunda: Materials Science and Engineering A, Vol. 393, 2005, Issues 1-2, p. 254-268.

[4] E. Dorazil: High Strength Austempered Ductile Iron, 2nd ed., Academia, Praha, 1991.

[5] B. V. Kovacs: Austempered ductile iron: fact and fiction, Modern Casting, 1990, p. 38-41.

[6] A. Trudel, M. Gagné: Canadian Metallurgical Quarterly, Vol. 36, 1997, Issue 5, p. 289-298.

[7] http://www.aditreatments.com/pdf/ADI%20in%20large%20diesel%20engines%20part%201.pdf, [04.08.2010].

[8] http://www.aditreatments.com/pdf/ADI%20in%20large%20diesel%20engines%20part%202.pdf, [04.08.2010].

[9] http://www.aditreatments.com/pdf/ADI%20solutions%20aid%20vehicle%20design.pdf, [04.08.2010].

[10] S. Massaggia: Procedia Engineering, Vol. 2, 2010, Issue 1, p. 1459-1476.

[11] ASTM E 647-08, Standard Test Method for Measurment of Fatigue Crack Growth Rates, In: Annual book of ASTM standards 2009.

[12] B. Stokes, N. Gao, P. A. S. Reed: Materials Science and Engineering: A, Vols. 445-446, 2007, p. 374-385.

[13] G. L. Greno, J. L. Otegui, R. E. Boeri: International Journal of Fatigue, Vol. 21, 1999, Issue 1, p. 35-43.